Proceedings of the 50th International School & Conference on the Physics of Semiconductors

Low Frequency Noise Properties of InAs/GaSb Superlattice

Ł. Ciura[a,*], P. Śliż[b], D. Jarosz[b,c], P. Krzemiński[b], M. Ruszała[b] and M. Marchewka[b]

[a] *Rzeszow University of Technology, W. Pola 2, 35-395 Rzeszow, Poland*
[b] *University of Rzeszow, Institute of Materials Engineering, Center for Microelectronics and Nanotechnology, al. Rejtana 16c, 35-959 Rzeszow, Poland*
[c] *International Research Centre Magtop, Institute of Physics, Polish Academy of Sciences, al. Lotników 32/46, 02-668 Warsaw, Poland*

Doi: 10.12693/APhysPolA.142.621 *e-mail: lciura@prz.edu.pl

The paper reports $1/f$ noise properties of InAs/GaSb superlattice as a function of voltage bias and temperature. Noise measurements were compared with standard transport characteristics: mobility and carrier concentration. Interestingly, while these standard characteristics of the two samples are comparable, the $1/f$ noise is substantially different. The results suggest that low-frequency noise is a more sensitive electronic transport characterization tool than standard techniques based on average current/voltage analysis.

topics: $1/f$ noise, noise measurements, InAs/GaSb superlattice

1. Introduction

In infrared (IR) detectors, noise has a significant practical meaning because it influences detectivity [1]. The $1/f$ noise is a common phenomenon in IR devices [2–5], which reduces detectivity in the low frequency range. The $1/f$ noise reduction is becoming an important goal in the development of better and better devices. One of the first steps in this optimization process is to determine the origin of 1/f noise in the constituent layers of IR detectors. Among the new materials for infrared detectors, superlattice (SL) materials have promising parameters that allow them to compete with HgCdTe.

This article investigates the correlation between $1/f$ noise and the basic characteristics of electronic transport (mobility and carrier concentration) for InAs/GaSb SL.

2. Samples and measurements

In this work, two samples made from I119 and I120 wafers were investigated. The SLs have been grown on GaAs:Un (100) $\pm 0.5^\circ$ substrates using a solid-source Riber Compact 21T (III-V) dual-zone molecular beam epitaxy system, equipped with valved arsenic and antimonic cracker, i.e., VAC 500 and VCOR 300, respectively. An arsenic pyrometer was used to measure the temperature of the substrate. The substrate rotation speed during growth was set to 10 rpm. The substrate temperature ramp rate was 10°C/min during the heat-up and 20°C/min during the cool-down processes. After the deoxidation of GaAs, approximately 500 nm of GaAs was applied at a temperature of 585°C to refresh the surface of the substrate. The 300 repetitions of non-intentionally doped InAs (3 nm)/GaSb (3 nm) were made. After applying the InAs layer, the surface was wetted with antimony for 4 s, while after applying the GaSb layer, the surface was wetted with arsenic for 2 s. The samples were cooled in an antimony atmosphere to 250°C. Figure 1 shows the $2\theta/\omega$ curves measured for InAs/GaSb SL by high-resolution X-ray diffraction (HRXRD) with the Malvern Panalytical diffractometer with Cu K (α_1) radiation ($\lambda = 1.540598$ Å).

The $2\theta/\omega$ scan was performed around the GaAs (004) reflex. For both samples, the highest intensity and narrowest peak are from the GaAs substrate. In addition, for the measured $2\theta/\omega$ curve of the analyzed structure, peaks of SL up to -3 and $+3$ of the order were observed. This proves that the SL crystals are of good quality. It also confirms the constancy of period thickness during growth.

In Fig. 1, the mean SL period of the I119 and I120 samples is 6.44 nm and 6.45 nm, respectively. Furthermore, the thicknesses of the individual SL layers in both samples were estimated and are listed in Table I.

Perpendicular lattice mismatch $(\Delta a/a)\perp$ between the buffer layer and the zero-order satellite peak of -5602 and -5322 ppm occurs for I119 and I120 samples.

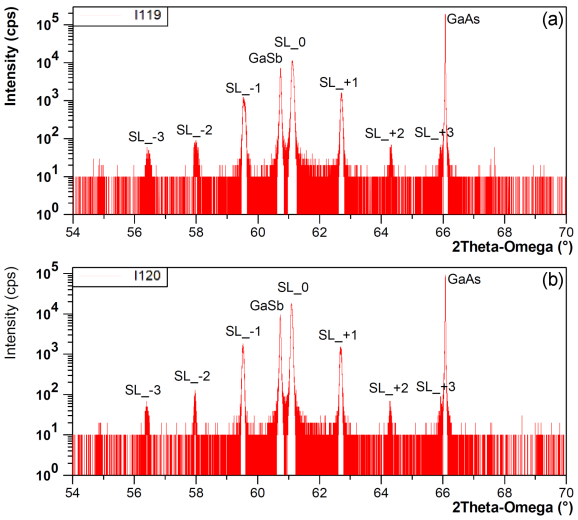

Fig. 1. The $2\theta/\omega$ curve measured for InAs/GaSb SLs (I119 and I120) by high-resolution X-ray diffraction.

TABLE I

The average thickness of the individual superlattice layers in the period.

	I119	I120
GaSb	2.95 nm	2.95 nm
InSb-like	0.34 nm	0.35 nm
InAs	2.90 nm	2.95 nm
GaAs-like	0.26 nm	0.25 nm

The Ecopia HMS-5000 Hall Measurement System was used to determine the concentration and horizontal mobility of carriers as a function of temperature in the investigated samples with the van der Pauw method. The samples were square/rectangular shapes with sizes 6.5×6.0 mm^2 and 6.2×6.2 mm^2 for samples I119 and I120, respectively. Indium electrical contacts were made at each corner of the samples by iron soldering. Before applying indium at the contact points, scratches were made with a scalpel on the sample surface. The contacts were soldered with a tip temperature of 200°C for 15–20 s for each contact. Additional smoothing of the tip contact surface for samples I119 and I120 was performed, with, respectively, the temperature of 156 °C and 158°C and the time of 5 s and 30 s. The samples were mounted on the cold finger of a sample holder and connected to the measurement setup using gold-plated spring probes. Measurements were made as a function of temperature from 80 to 300 K with an increment of 10 K at an excitation current of 50 μA.

The low frequency noise was measured with the setup presented in Fig. 2 for the same samples that were used for mobility and carrier concentration measurements. The structures were biased with

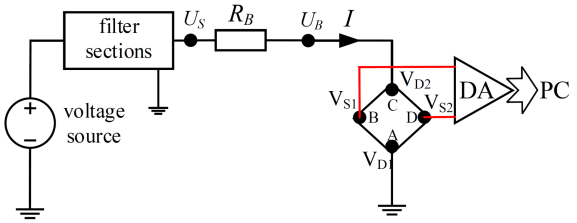

Fig. 2. Four-point probe noise measurements setup.

the constant current I from a quasi-current source containing a low-noise voltage source and the resistance R_B, which is significantly larger ($R_B \gg R$) than the resistance R measured at the same contacts. The structure resistance is obtained indirectly from the measured source voltage U_S and the bias voltage U_B as $R = U_B/I = U_B/((U_S - U_B)/R_B)$. The bias current is fed to one pair of terminals (V_{D1} and V_{D2}) called driving contacts, while at another pair of contacts (V_{S1} and V_{S2}), voltage fluctuations with a differential amplifier ($V_{S2} - V_{S1}$) are measured. This signal path is parallelized (not shown in Fig. 2) to benefit from the cross-correlation method [6], which reduces the power spectral density of the uncorrelated voltage noise of the two amplifiers to approximately 10^{-18} V^2/Hz. This four-point measurement configuration reduces the influence of contact noise because the bias current does not flow into the high-impedance input (100 MΩ) of the differential amplifier. It should be noted that voltage fluctuations occurring at driving contacts are suppressed because they are common components of the signals V_{S2} and V_{S1} provided to the differential amplifier. Consequently, measured $1/f$ noise should be related to the SL properties, not electrical contacts' properties.

3. Results

Figure 3 shows the carrier concentration and horizontal mobility measured for the I119 and I120 samples as a function of temperature.

In the low-temperature region ($T < 230$ K), the carrier (electron) concentrations are about 2.1×10^{16} cm^{-3} and 2.5×10^{16} cm^{-3} for I119 and I120, respectively. In the high-temperature region, both concentrations increase, probably due to an increase in intrinsic carrier concentration. Sample I120, with higher non-intentional doping, has slightly lower carrier mobility, which is expected when mobility is limited by ionized impurity scattering [7]. Moreover, both mobilities increase with temperature. This trend is also a sign of the impurity scattering mechanism. However, the T-dependence observed in the mobility ($\mu \propto T^{0.25}$) is far from $\mu \propto T^{1.5}$ dependence expected for the mobility of carriers in bulk semiconductors limited by this scattering mechanism [7]. The sheet resistance for both samples at

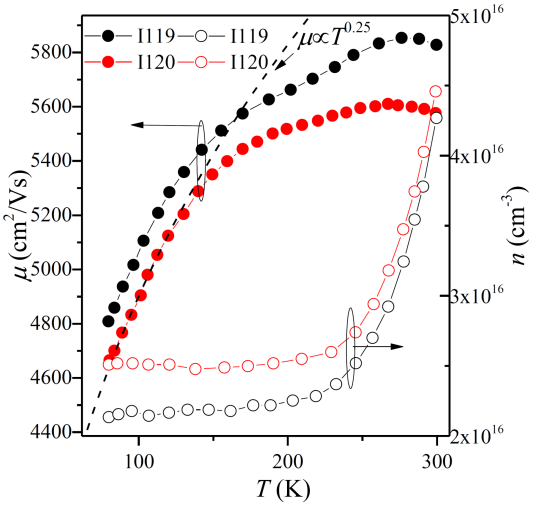

Fig. 3. Carrier concentration and horizontal mobility measured as a function of temperature for I119 and I120.

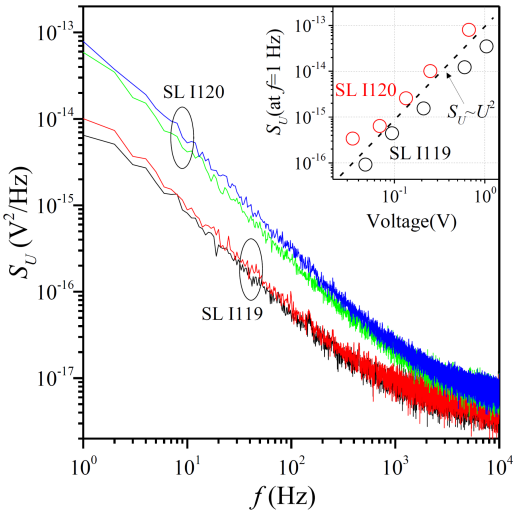

Fig. 4. Power spectral densities measured at room temperature for samples biased with current I = 2 mA. Power spectral densities were measured at different sensing contacts (AC and BD) for each sample. In the inset, the $1/f$ magnitude at $f = 1$ Hz is shown as a function of the voltage bias.

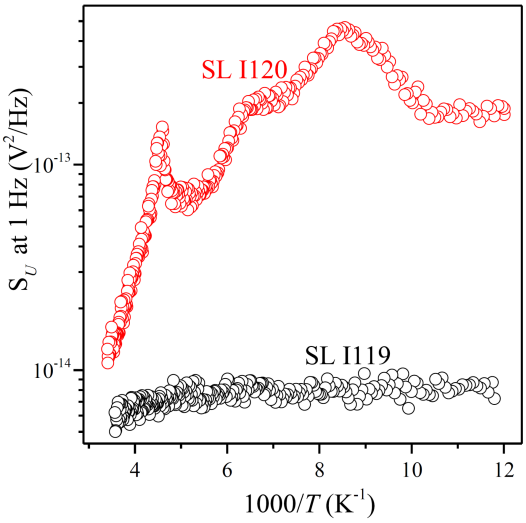

Fig. 5. Power spectral density S_U at 1 Hz as a function of temperature for samples SL I119 and SL I120.

room temperature is 132 Ω/sq. At $T = 80$ K, the sheet resistance is 266 Ω/sq and 308 Ω/sq for I120 and I119, respectively.

In Fig. 4, the power spectral densities, S_U, measured at room temperature for both SL structures biased with current $I = 2$ mA, are shown. In this experiment, two measurements were made at the diagonal contacts, AC and BD, for each sample. Changing the contacts' role from driving to sensing should not change the measured noise magnitude if noise originated from resistance fluctuations [8–10]. This so-called reciprocity rule holds for both SL structures, which means that: (i) contact noise does not contribute to the total measured noise, (ii) fluctuations originate from mobility or carrier concentration. The $1/f$ noise magnitude as a function of voltage bias is shown in the inset in Fig. 4. For both structures, $1/f$ noise magnitude exhibits $S_U \propto U^2$ dependence, which is typical for ohmic samples. The relative $1/f$ noise, $C_{1/f} = S_U/U^2$, is higher for I120.

In Fig. 5, $1/f$ noise magnitudes (S_U at $f = 1$ Hz) are shown as a function of temperature for both considered SL samples. Because the same bias current $I = 1.5$ mA was applied, and the samples have comparable sheet resistances, S_U can be used for noise properties comparison without further normalization of the results.

As can be seen, SL I120 has significantly higher 1/f noise than SL I119, especially in the low-temperature range. For SL I120, the noise magnitude decreases with increasing temperature, whereas for SL I119, it is almost temperature-independent.

The most interesting observation is that the difference in $1/f$ noise magnitude of both samples is much more substantial than a difference in mobility or carrier concentration. The difference between the electron mobility of I119 and I120 SL is only a few percent. The difference in carrier concentrations is about 25% (at a low temperature). In the low-temperature region, the difference between the $1/f$ noise magnitudes of samples is more substantial and exceeds one order of magnitude. On this basis, it can be claimed that the noise measurement is more sensitive to local effects [9] (i.e., high local inhomogeneous current) than average quantities such as sheet resistance, which is comparable for both samples. More studies are needed, including a batch of samples with different doping and mobility, to reveal the origin of the fluctuations.

4. Conclusions

InAs/GaSb SL samples with similar sheet resistance, mobility, and carrier concentration have substantially different $1/f$ noise properties, especially in the low-temperature region. The measured $1/f$ noise is attributed to resistance fluctuations of the SL structure, not the metal-SL interface, because differential noise measurements with the four-point probe were used, which suppressed contact noise.

Acknowledgments

This project is financed by the Minister of Education and Science of the Republic of Poland within the "Regional Initiative of Excellence" program for years 2019–2023, project number 027/RID/2018/19, amount granted 11 999 900 PLN.

This work was supported by the International Centre for Interfacing Magnetism and Superconductivity with Topological Matter project, carried out within the International Research Agendas program of the Foundation for Polish Science co-financed by the European Union under the European Regional Development Fund.

This research was partially co-financed by the National Centre for Research and Development (NCBR), under project number POIR.04.01.04-00-0123/17.

References

[1] A. Rogalski, *Infrared and Terahertz Detectors*, 3rd Ed., CRC Press, Boca Raton 2019.

[2] K. Czuba, L. Ciura, I. Sankowska, E. Papis-Polakowska, A. Jasik, *Sensors* **21**, 7005 (2021).

[3] Ł. Ciura, M. Kopytko, P. Martyniuk, *Sensors Actuat. A: Phys.* **305**, 111908 (2020).

[4] Ł. Ciura, A. Kolek, K. Michalczewski, K. Hackiewicz, P. Martyniuk, *IEEE Trans. Electron Devices* **67**, 3205 (2020).

[5] Ł. Ciura, A. Kolek, J. Jureńczyk, K. Czuba, A. Jasik, I. Sankowska, J. Kaniewski, *Opt. Quantum Electron.* **50**, 36 (2017).

[6] F. Crupi, G. Giusi, C. Ciofi, C. Pace, *IEEE Trans. Instrum. Meas.* **55**, 1143 (2006).

[7] D. Chattopadhyay, H.J. Queisser, *Rev. Mod. Phys.* **53**, 745 (1981).

[8] L.K.J. Vandamme, G. Leroy, *Fluct. Noise Lett.* **06**, L161 (2006).

[9] T. Ciuk, Ł. Ciura, P.P. Michałowski et al., *Phys. E Low-dimen. Syst. Nanostruct.* **142**, 115264 (2022).

[10] L. Ciura, A. Kolek, D. Smoczyński, A. Jasik, *Bull. Pol. Acad. Sci. Tech. Sci.* **68**, 135 (2020).